Boron Oxide Oligomer Collision-Induced Dissociation: Thermochemistry, Structure, and Implications for Boron Combustion

Dilrukshi Peiris, Adam Lapicki, and Scott L. Anderson*
Chemistry Department, University of Utah, Salt Lake City, Utah 84112

Robert Napora, Doug Linder, and Michael Page*
Chemistry Department, North Dakota State University, Fargo, North Dakota 58105

Received: July 2, 1997; In Final Form: September 26, 1997[⊗]

This paper presents a comprehensive collision-induced dissociation and ab initio study of small boron oxide cations, $B_nO_m^+$, motivated by a need for more accurate and reliable structural and thermodynamic information on both neutral and ionic boron oxides. Absolute fragmentation cross sections were measured for all observable $B_nO_m^+$ ($n < 4$, $m < 5$) parent ions at center-of-mass collision energies ranging from 0.08 to 10 eV. Quantitative dissociation thresholds, generated from the experimental data by correcting for the collision energy spread resulting from the beam energy distribution and the thermal motion of the target gas, are compared to ab initio dissociation energies determined from Gaussian-2 calculations.

I. Introduction

This paper presents a comprehensive collision-induced dissociation (CID) and ab initio study of small boron oxide cations, $B_nO_m^+$, motivated by a need for more accurate and reliable structural and thermodynamic information on both neutral and ionic boron oxides. This work complements other ongoing ab initio calculations by Page and co-workers[1] involving neutral boron oxide clusters and provides many points of comparison between experiment and theory. In addition, the results of the CID study are important in interpretation of boron oxide cluster chemistry work at the Utah lab.

In combustion of boron or boron rich fuels and propellants, boron-oxide chemistry plays two important roles. Boron particles are naturally coated with a passivating layer of the oxide, which may be at least partly converted to hydroxide (i.e., boric acid) depending on humidity and temperature. As the particles heat up in a combustion environment, the oxide layer retards boron ignition until it is removed. Oxide layer volatilization occurs by evaporation at high temperatures, but the potential exists to accelerate ignition by chemical removal at lower temperatures. Boron oxide properties are also important in achieving energy release in the post-oxidation chemistry. In particular, full energy release occurs only if the gaseous $B_nO_mH_l$ oxidation products condense to thermodynamically stable products such as $B_2O_3(l)$, rather than remain as $(B_nO_mH_l)_k$ oligomers. Clearly, the chemistry and thermodynamics of small $B_nO_mH_l$ species are important in this process.

A promising strategy to enhance boron combustion is to fluorinate the hydrocarbon components of a boron-containing propellant. Decomposition of the hydrocarbon releases HF, which can attack the boron or boron oxide particle surfaces. Because boron has a high affinity for fluorine and F is isoelectronic with OH, fluorine will tend to displace OH or O from oxides, forming stable $B_nO_mH_lF_k$ species. And because fluorine compounds of boron are more volatile than oxides or hydroxides, HF attack should tend to volatilize the oxide layer. Indeed FBO is observed as the major product of HF attack on small boron oxide cluster ions,[2] in accord with modeling predictions based on thermodynamic considerations.[3,4]

In the course of the HF/boron oxide cluster study, we found substantial uncertainties in the thermodynamics reported for small $B_nO_mH_lF_k$ compounds. Much of the thermochemistry is based on low-level ab initio or semiempirical quantum chemistry calculations, which are not expected to be very reliable. Recent and ongoing high-quality ab initio calculations[1,5−7] are improving the situation dramatically; however, there is little experimental data available to test the accuracy of the calculations. The experimental results reported here largely validate the accuracy of the theoretical calculations, while the calculated results provide considerable insight into the interpretation of our experiments.

One major puzzle remains. In the course of an experimental study of the reaction of HF with $B_nO_m^+$ clusters,[2] we observed a reaction producing FBOH. From the energy dependence of the cross section for this reaction, it clearly is exothermic, and based on estimates of the thermodynamics for $B_nO_m^+$, we predicted that FBOH should have a ΔH_f no higher than −194 kcal/mol. This is 80 kcal/mol more stable than predicted by the calculations of Page and co-workers[1] and Soto,[6] and this discrepancy is far outside the usual uncertainties expected for calculations of that quality. Our ΔH_f was based in part on *estimates* for the thermochemistry of the larger $B_nO_m^+$ species, and this seemed to be a likely source of the disagreement. One motivation for the present CID study was, therefore, to determine the stabilities of these species directly. Despite overall good agreement between our experiments and the calculations, this particular controversy remains unresolved.

II. Methods

Experimental Section. *Apparatus*. The cluster beam instrument and operating procedures used for these experiments have been described in detail elsewhere.[2,8,9] Briefly, boron oxide cluster ions are generated by 12 keV argon atom bombardment[10] of a film of vitreous $^{10}B_2O_3$ maintained near its melting point. The nascent $B_xO_y^+$ cluster ions are collected by a radio frequency (rf) octapole ion guide and cooled to near room temperature by storage in a labyrinthine rf trap containing ∼0.01 Torr of helium buffer gas. The reactant cluster ion size and composition is selected using a quadrupole mass filter, and then the beam is injected into another octapole ion guide system where scattering is carried out. The octapole sets the collision energy and guides the ions through a collision cell filled with either xenon or argon to a typical pressure of 1×10^{-5} Torr. For these experiments we need single-collision conditions, and this was checked by measuring cross sections over a range of

[⊗] Abstract published in *Advance ACS Abstracts,* November 15, 1997.

S1089-5639(97)02157-9 CCC: $14.00

xenon/argon pressures. Fragment ions and the remaining parent ions are collected by the octapole, mass analyzed by a second quadrupole mass spectrometer, and counted.

Sample Preparation. Isotopically purified (94.11 At.% of ^{10}B) boron oxide (B_2O_3) powder (Eagle-Pitcher) was sprinkled on a stainless steel substrate, and then heated in a furnace at 650 °C for about 4 h in an oxygen environment to produce a vitreous film. Because boron oxide is found to be highly hygroscopic, the sample is maintained at 350−450 °C in the high-vacuum cluster source chamber.

Calculations. The ab initio calculations were performed using the Gaussian-2(G2) methodology proposed by Pople and co-workers.[11] Briefly, single-point energy calculations are performed at MP2(full)/6-31G(d) optimized geometries with a series of additive corrections designed to approximate a single calculation at the QCISD(T)/6-311+G(3df,2p) level. In particular, G2 Energies are obtained by adding corrections for basis set incompleteness and higher level electron correlation to energies determined at the MP4SDTQ/6-311G(d,p) level, as in eq 1

$$E[\mathrm{G2}] = E[\mathrm{MP4SDTQ/6\text{-}311G(d,p)}] + \Delta(+) + \Delta(\mathrm{2df}) + \Delta(\mathrm{QCI}) + \Delta + \Delta(\mathrm{HLC}) + \Delta(\mathrm{ZPE}) \quad (1)$$

where

$$\Delta(+) = E[\mathrm{MP4SDTQ/6\text{-}311+G(d,p)}] - E[\mathrm{MP4SDTQ/6\text{-}311G(d,p)}] \quad (2)$$

$$\Delta(\mathrm{2df}) = E[\mathrm{MP4SDTQ/6\text{-}311G(2df,p)}] - E[\mathrm{MP4SDTQ/6\text{-}311G(d,p)}] \quad (3)$$

$$\Delta(\mathrm{QCI}) = E[\mathrm{QCISD(T)/6\text{-}311G(d,p)}] - E[\mathrm{MP4SDTQ/6\text{-}311G(d,p)}] \quad (4)$$

$$\Delta = E[\mathrm{MP2/6\text{-}311+G(3df,2p)}] - E[\mathrm{MP2/6\text{-}311G(2df,p)}] - E[\mathrm{MP2/6\text{-}311+G(d,p)}] + E[\mathrm{MP2/6\text{-}311G(d,p)}] \quad (5)$$

$$\Delta(\mathrm{HLC}) = -0.00019n_a - 0.00481n_b \quad (6)$$

$$\Delta(\mathrm{ZPE}) = 0.8929\ \mathrm{ZPE[HF/6\text{-}31G(d)]} \quad (7)$$

In the above equations, $\Delta(+)$ corrects for the effect of diffuse functions, $\Delta(\mathrm{2df})$ for the effect of higher polarization functions, and $\Delta(\mathrm{QCI})$ for the effect of electron correlation beyond fourth order. The nonadditivity caused by the assumption of separate basis set extensions in the original G1 method is corrected by the Δ-term. $\Delta(\mathrm{HLC})$ (in hartrees) is an empirical correction based on the number of a (alpha) and b (beta) valence electrons (n_a or n_b), to bring calculated atomization energies into agreement with well-established experimental results for 55 molecules. The zero-point energy (ZPE) correction term is computed by scaling the zero-point energy (harmonic vibrational frequencies) calculated at the HF/6-31G(d) level.

To obtain theoretical heats of formation, we compute the atomization energies at the G2 level of theory and combine these with the following experimental heats of formation for the atoms: (H) = 52.1 kcal/mol,[12] (F) = 18.9 kcal/mol,[12] (O) = 59.6 kcal/mol,[12] and (B) = 137.4 kcal/mol.[13] The value used here for the heat of formation of boron atom, which is higher than the JANAF recommendation[12] of 133.8 ± 3 kcal/mol, is supported by the photoionization study of Ruscic et al.[14] and was adopted by Schlegel and Harris[15] in their recent G2 study of BH_mCl_n.

The electronic structure calculations employed in the G2 method are all based on a single-configuration reference wave function. Although this is not expected to be a problem for the thermochemistry calculations, it represents a potential problem in the determination of isomerization barriers, where there may be significant electron unpairing. Transition-state structures—determined at the MP2 level of theory in the G2 method—may be unreliable in such cases. For this reason, the complete active space self-consistent field (CASSCF)[16] method has been used for some of the geometry optimizations as a check. All CASSCF calculations use the MESA[17] system of programs.

III. Results

Reactant Beam Kinetic Energy Distribution. Accurate CID threshold determinations require a narrow and well-defined kinetic energy distribution for the primary beam. This is measured by retarding potential analysis and controlled by fine adjustments of the focusing lens system. The beam energy distribution is obtained by fitting the retarding curve to a 3-parameter asymmetric Lorentzian function:

$$F(x) = \frac{A}{\{1 + [(x - E_0)/b]^2\} \exp(x - E_0)^c}$$

A is simply an intensity factor, E_0 represents the shift in average beam energy relative to the nominal LAB KE of the ions, b determines the energy width, and c is an asymmetry parameter (usually quite small). Typical distributions have LAB frame energy spreads of 0.25 eV, contributing 0.15 to 0.2 eV to the collision energy distribution.

Reaction Cross Sections and Branching Patterns. Absolute fragmentation cross sections were measured for all observable $B_nO_m^+$ ($n < 4$, $m < 5$) parent ions at center-of-mass collision energies ranging from 0.08 to 10 eV. Cross sections are shown for all significant fragmentation channels in Figure 1. Fragmentation in collision with both argon and xenon was studied and the best results are presented. Xenon generally seems to be a more efficient target gas; however, argon was found to give sharper threshold behavior for several of the smallest cluster ions, presumably because the kinematics result in better collision-to-internal energy transfer.

Extracting CID Thresholds. To obtain quantitative dissociation thresholds from the experimental data we need to correct for the collision energy spread resulting from the beam energy distribution and the thermal motion of the target gas. This was done by a standard convolution and fitting approach that has been described in detail previously.[18] Briefly, the cross sections in the threshold region were modeled using an assumed "true" cross section functional form that has been widely used in the scattering community:

$$\sigma(E_{\mathrm{avail}}) = \frac{A(E_{\mathrm{avail}} - E_0)^n}{E_{\mathrm{avail}}}$$

where A is a normalization factor; E_0 is the dissociation threshold; and n is an adjustable parameter that varies the curvature of the function, physically related to the energy transfer efficiency. E_{avail} is the total energy available to drive fragmentation, assumed in this case to be the collision energy plus thermal, vibrational, and rotational energy of the cluster ion reactant.

This trial function is convoluted (through a Monte Carlo simulation) with the kinetic energy distribution of the primary cluster ions, the translational energy distribution of the target gas, and the distribution of vibrational and rotational energy of cluster ions. The vibrational energy distribution has been calculated assuming that the clusters are at 400 K, using

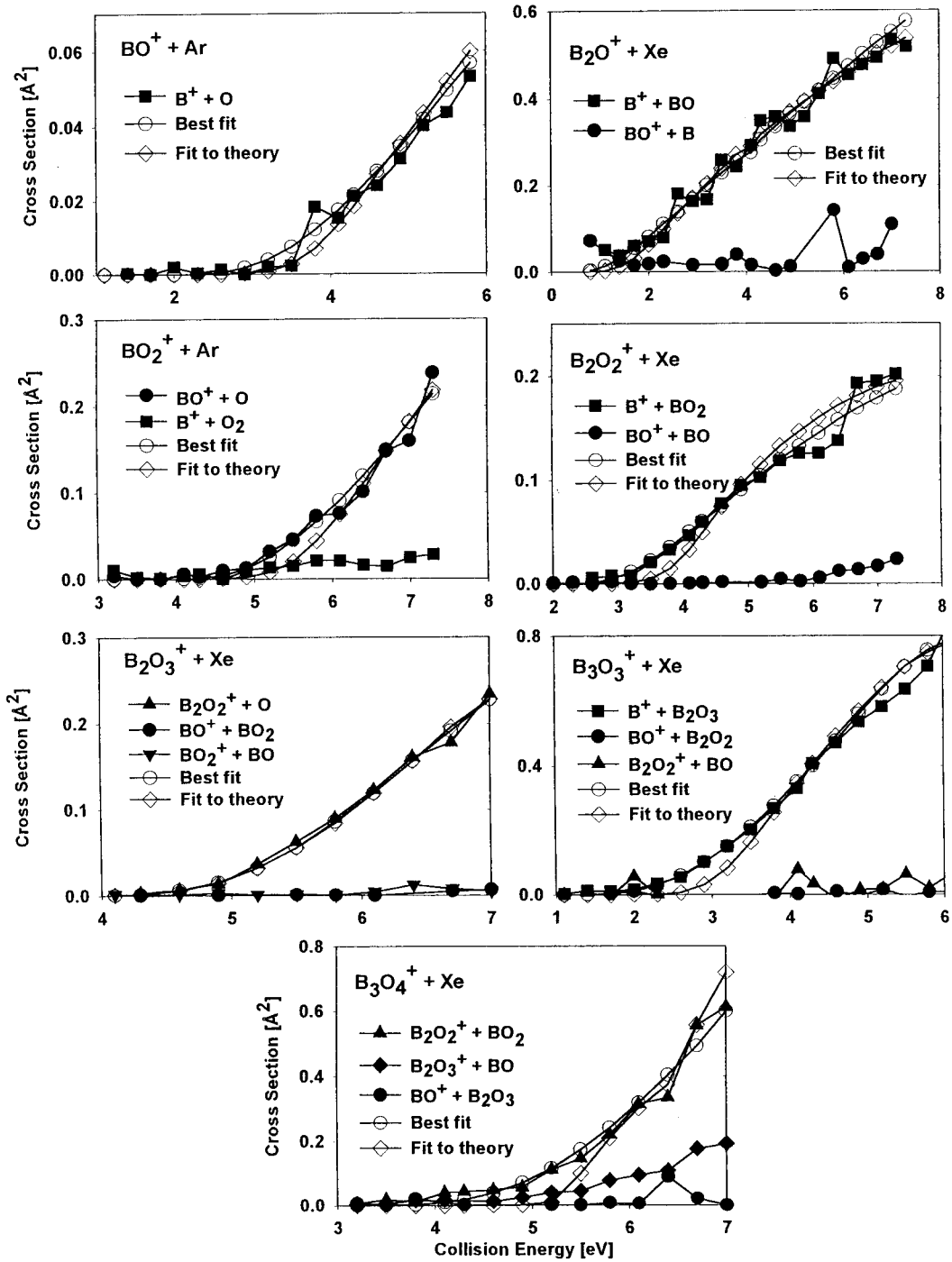

Figure 1. Cross sections for all significant fragmentation channels along with the best fits for the lowest energy dissociation pathways of boron oxide cluster cations.

vibrational frequencies from the ab initio calculations. The parameters n and E_0 are optimized until a best fit is obtained. To check for the possibility of kinetic shifts, RRKM theory[19] was used to calculate dissociation rates as a function of energy, using the ab initio vibrational frequencies. For the cluster size range of interest here, the kinetic shifts are found to be negligible.

Fitting was attempted only for the lowest energy fragmentation channel for each reactant cluster ion. In principle, additional thermochemical information can be extracted from the higher energy dissociation channels; however, this analysis is complicated by a difficult-to-estimate competitive kinetic shift factor.

The best fits for the lowest energy fragmentation channels are shown in Figure 1. The curves labeled "Best fit" are best free fits to the data, and the extracted E_0 values are the experimental estimates for dissociation energies. We also plot "Fit to Theory" curves. These are fits based on E_0 values calculated using the G2 heats of formation with only the n parameter adjusted in an attempt to fit the data. These are plotted to show the cases for which the experiment and theory are or are not in agreement. The fit thresholds (E_0) and n parameters for the lowest energy dissociation channel of each cluster for both types of fittings are given in Table 1, along with the ab initio dissociation thresholds. To show the strong dependence of the dissociation threshold on cluster composition, Figure 2 gives experimental and ab initio dissociation energies as a function of B:O stoichiometry.

Calculations. Table 2 lists the geometries fully optimized at the MP2(full)/6-31G(d) levels for all the compounds. Table

TABLE 1: Best Fit Parameters (n) and Best Fit Dissociation Energy Thresholds (E_0) of Boron Oxide Cluster Ions

	best fit		fit to theory[a]	
dissociation channel	n	E_0	n	E_0
$BO^+ \rightarrow B^+ + O$	1.90	2.75 ± 0.6	1.35	3.60
$B_2O^+ \rightarrow B^+ + BO$	1.80	1.30 ± 0.5	1.40	1.90
$BO_2^+ \rightarrow BO^+ + O$	1.60	4.75 ± 0.6	1.05	5.60
$B_2O_2^+ \rightarrow B^+ + BO_2$	1.30	3.15 ± 0.2	1.05	4.10
$B_2O_3^+ \rightarrow B_2O_2^+ + O$	1.64	5.10 ± 0.2	1.70	5.09
$B_3O_3^+ \rightarrow B^+ + B_2O_3$	2.05	2.00 ± 0.2	1.05	3.2
$B_3O_4^+ \rightarrow B_2O_2^+ + BO_2$	2.10	4.25 ± 0.5	1.1	6.4

[a] E_0 values from G2 heats of formation.

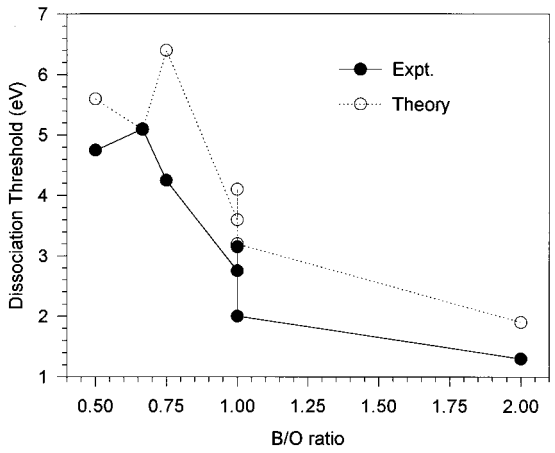

Figure 2. The cluster cation's stability as a function of boron-to-oxygen ratio.

3 lists the G2 energies, the theoretical atomization energies at 0 K, and theoretical heats of formation at 298 K. The heats of formation were obtained from the G2 energies, the Hartree−Fock thermal corrections, and the heats of formation of the atoms. Available experimental heats of formation are also displayed in Table 3 for comparison.

IV. Discussion

Isomer Distributions in the Cluster Ion Beam. As shown in Table 3, a number of the boron oxide cluster ions have isomers lying close in energy to the ground state. Quantitative comparison of the experimental dissociation thresholds with calculated dissociation energies requires that we know what cluster isomers are present in our ion beam. CID signal in the threshold energy range (i.e., the first appearance of fragment ions), as well as the dissociation threshold extracted by fitting the signal, are inherently most sensitive to the least stable isomer present in significant concentration (>1−2%). In cases such as carbon cluster ions, where linear and cyclic isomers have very different reactivity at low collision energies, we can easily determine the ratio of isomers. For the boron oxides we do not have a good "titration" reaction and have to estimate the isomer distribution from theoretical considerations.

Our cluster ions are made by particle sputtering, which produces a distribution of cluster sizes with very high internal temperatures. These hot cluster ions initially cool by evaporation, then are actively cooled by $>10^5$ collisions with helium buffer gas over a ~1 s period. Based on previous tests, we are confident that the clusters have internal temperatures near room temperature at the exit of the cooling trap.

In a slow cooling process such as we use, we believe that the final distribution of isomers can be estimated as follows. Consider the case of a ground-state isomer separated from a higher energy isomer by an activation barrier. Initially, the internal temperature is sufficiently high that isomerization over the barrier is rapid. In this high-temperature regime, the ratio of the two isomers is determined by the ratio of the density of states (DOS) in the two isomer wells. As the clusters cool, the DOS corresponding to the high-energy isomer will decrease

TABLE 2: MP2/6-31G*(full) Structural Parameters for $B_xO_y^+$ Isomers

molecule	structure	2S + 1	symm	geom (Å and deg)
BO				
BO^+(1-SG)	B=O	1	$C_{\infty v}$	r(BO) = 1.238
B_2O				
BOB^+	B−O−B	2	$D_{\infty h}$	r(BO) = 1.329
BOB^+(ring)		2	C_{2v}	r(BO) = 1.342
				r(BB) = 1.788
				α(BOB)=83.5
BBO^+	B−B=O	2	$C_{\infty v}$	r(BB) = 1.690
				r(BO) = 1.192
BO_2				
OBO^+(trip)	O−B−O	3	$D_{\infty h}$	r(BO) = 1.272
OBO^+(sing)	O−B−O	1	$D_{\infty h}$	r(BO) = 1.301
OBO^+(ring, trip)		3	C_{2v}	r(BO) = 1.417
				r(OO) = 1.456
				α(OBO) = 61.8
B_2O_2				
$BOBO^+$	B−O−B=O	2	$C_{\infty v}$	$r(B_1O_1)$ = 1.237
				$r(O_1B_2)$ = 1.389
				$r(B_2O_2)$ = 1.209
$BOOB^+$(ring, D2h)		2	D_{2h}	r(BO) = 1.384
				r(BB) = 1.651
				α(OBO) = 106.7
$BOOB^+$(ring, C2v)		2	C_{2v}	$r(B_1O)$ = 1.341
				r(BB) = 1.652
				$\alpha(OB_1O)$ = 113.0
				$r(B_2O)$ = 1.443
				$\alpha(OB_2O)$ = 101.6
$OBBO^+$	O=B−B=O	2	$D_{\infty h}$	r(BO) = 1.235
				r(BB) = 1.640
B_2O_3				
$OBOBO^+$(asym)	O=B−O=B−O	2	$C_{\infty v}$	$r(O_1B_1)$ = 1.211
				$r(B_1O_2)$ = 1.380
				$r(O_2B_2)$ = 1.244
				$r(B_2O_3)$ = 1.324
$B_3O_3^+$				
$OBBOBO^+$	O=B−B−O−B=O	1	$C_{\infty v}$	$r(O_1B_1)$ = 1.218
				$r(B_1B_2)$ = 1.637
				$r(B_2O_2)$ = 1.239
				$r(O_2B_3)$ = 1.384
				$r(B_3O_3)$ = 1.210
$BOBOBO^+$	B−O−B−O−B=O	1	$C_{\infty v}$	$r(B_1O_1)$ = 1.431
				$r(O_1B_2)$ = 1.266
				$r(B_2O_2)$ = 1.253
				$r(O_2B_3)$ = 1.370
				$r(B_3O_3)$ = 1.211
$OB-BOOB^+$		1	C_{2v}	$r(O_1B_1)$ = 1.215
				$r(B_1B_2)$ = 1.653
				$r(B_2O)$ = 1.501
				$r(B_3O)$ = 1.315
				$r(B_2B_3)$ = 1.660
				α(BBO) = 131.2
				$\alpha(OB_3O)$ = 118.5
$B_3O_4^+$				
$OBOBOBO^+$	O=B−O−B−O−B=O	1	$D_{\infty h}$	$r(O_1B_1)$ = 1.211
				$r(B_1O_2)$ = 1.371
				$r(O_2B_2)$ = 1.253
$OBO-BOOB^+$		1	C_s	$r(O_1B_1)$ = 1.212
				$r(B_1O_2)$ = 1.369
				$r(O_2B_2)$ = 1.290
				$r(B_2O_3)$ = 1.529
				$r(B_2O_4)$ = 1.512
				$r(O_3B_3)$ = 1.309
				$r(O_4B_3)$ = 1.312
				$r(B_2B_3)$ = 1.675
				$\alpha(O_1BO_2)$ = 179.3
				$\alpha(B_1O_2B)$ = 139.7
				$\alpha(O_2BO_3)$ = 133.8
				$\alpha(O_2BO_4)$ = 130.0
				$\alpha(O_2B_2B)$ = 178.3
				$\alpha(OB_3O)$ = 119.5

TABLE 3: G2 Heats of Formation (in kcal/mol) for $B_xO_y^+$ Isomers

molecules	G2 energy (0 K) (hartrees)	$\Delta H°_{atom,0}$	$\Delta H°_{f,298}$ (calc)	$\Delta H°_{f,298}$ (exp)
B	−24.602 036			137.4
B^+	−24.300 664		326.5	328.8
O	−74.982 030			59.6
BO				
BO^+(singlet)	−99.412 12	81.2	304.0	300 299
B_2O				
BOB^+	−124.260 98	236.1	286.0	
BOB^+(ring)	−124.250 62	229.6	292.0	
BBO^+	−124.247 71	227.8	294.0	
BO_2				
OBO^+(triplet)	−174.598 98	209.8	234.4	240
OBO^+(singlet)[a]	−174.576 37	195.6	248.2	
OBO^+(ring, trip)[a]	−174.500 26	147.8	295.8	
B_2O_2				
$BOBO^+$	−199.527 66	414.7	165.7	
$BOOB^+$(ring, D_{2h})[a]	−199.501 17	398.1	181.7	
$BOOB^+$(ring, C_{2v})	−199.500 23	397.5	182.3	
$OBBO^+$ [a]	−199.454 55	369.6	212.8	
B_2O_3				
$OBOBO^+$(asym)	−274.710 07	540.5	98.6	110
$B_3O_3^+$				110
$OBBOBO^+$	−299.597 37	719.5	56.3	
$BOBOBO^+$	−299.576 53	706.4	69.7	
$OB-BOOB^+$	−299.555 19	693.0	82.2	
$B_3O_4^+$				
OBOBOBO	−374.836 86	881.0	−46.4	
OBO−BOOB[b]	−374.784 34	854.8	−21.5	

[a] Used MP2 frequencies. [b] G2(MP2) theory.

faster than that for the ground-state isomer, thus the distribution will shift toward the ground-state structure. This annealing process will continue until the internal energy drops below the barrier height, at which point the isomer distribution is frozen as the energy continues to drop. Helium was chosen as our buffer gas partly in consideration that many ineffective cooling collisions should anneal more completely than a smaller number of collisions with a more efficient buffer gas.

In this scenario, we would expect to see substantial contribution from a higher energy isomer only if the energy difference between isomers is small compared to the activation barrier to isomerization. In this case, the DOS for the higher energy isomer will still be comparable to that of the ground state at the energy where isomerization freezes out. The structures of the two isomers are also important, since this can affect the DOS ratio. For example, linear isomers will tend to have a higher DOS, and thus higher population, than cyclic isomers at the same internal energy.

To examine this possibility, we determined transition states for isomerization between the higher energy four-membered ring structures and the ground-state linear structures for both the $B_2O_2^+$ and $B_3O_3^+$ cases. Both reactions involve breaking a B−O σ-bond and a substantial increase in BO π-bonding. To describe these changes, transition-state structures were optimized using a three-electron, three-active orbital complete active space SCF wave function. In both cases the wave function at the transition state was dominated by a single-reference configuration, so the isomerization barriers were determined using the G2 method.

We calculated the densities of states and barrier crossing rates in both directions as a function of energy above the barrier, using ab initio vibrational frequencies and the RRKM program of Zhu and Hase.[19] The $B_2O_2^+$ ring-opening isomerization, which is 17.2 kcal/mol exothermic, has a barrier of 9.4 kcal/mol. We are thus interested in the DOS for the linear isomer 26.6 kcal/mol above its potential energy minimum compared to the DOS for the cyclic isomer just 9.4 kcal/mol above its potential energy minimum. The DOS ratio is even more favorable for annealing than might be expected from the isomer energy difference, because the linear ground isomer has four bending vibrational modes (two at 163.7 cm^{-1} and two at 436.1 cm^{-1}) that are below even the lowest frequency for the cyclic isomer (490.0 cm^{-1}). Two kcal/mol above the classical barrier, the DOS ratio is 3000:1 in favor of the ground-state isomer. Even 20 kcal/mol above the barrier, the DOS ratio is 1000:1, suggesting that a significant population of the higher energy cyclic isomer is very unlikely.

The $B_3O_3^+$ four-membered ring structure is even less likely to contribute, because the ring-opening isomerization is 26.5 kcal exothermic and has a barrier of only 3.2 kcal/mol. In addition, once again the ground state has a linear structure with more low-frequency vibrational modes. Although we have not done the calculations for the ring-opening isomerization of $B_3O_4^+$, it is just about as exothermic as that for $B_3O_3^+$ and likely also has a very small isomerization barrier.

Fragmentation Branching Ratios. In fragmentation reactions, two factors can control the branching between different possible fragment channels. In some cases, one might expect that the geometrical structure of the parent cluster ion would be reflected in the fragments, i.e., that fragmentation might occur by simple bond rupture, without rearrangement. This is particularly likely in high-energy CID, where the fragmentation time scale is short. In low-energy CID, such as our near-threshold work, the fragmentation time scale is long enough that rearrangement can occur prior to, or during, decomposition. In this case, the fragment branching is influenced strongly by the thermochemistry of the possible products, with the most stable products dominating.

On the basis of the available thermochemistry in the literature[2,5,6,20] and our ab initio calculations, it appears that product thermochemistry is the dominant factor for all but one of the boron oxide cluster ions we have examined. For BO^+, B_2O^+, $B_2O_2^+$, and $B_3O_3^+$, all clusters where the number of B atoms is equal to or greater than the number of O atoms in the parent cluster, the dominant fragmentation pathway is loss of B^+. This appears to reflect two factors: the low ionization energy of the boron atom and the relatively high stability of fragments with B_nO_{n+1} stoichiometry.

For the $B_2O_3^+$ parent cluster, the only important fragmentation channel is loss of O, yielding $B_2O_2^+$. Dissociation to $BO^+ + BO_2$, only 0.5 eV higher in energy, accounts for only a few percent of the products, even at energies well above threshold. $B_3O_4^+$, which also prefers to decompose to $B_2O_2^+$ (+ BO_2), produces a substantial branching to the nearly isoenergetic fragment pairs $B_2O_3^+ + BO$ and $BO^+ + B_2O_3$ that lie ~0.3 eV higher in energy.

An exception to control by fragment thermochemistry is BO_2^+. The dominant decomposition channel is to $BO^+ + O$, even though the $B^+ + O_2$ channel is ~1.6 eV lower in energy. This presumably reflects either a barrier or a dynamical bottleneck that inhibits passage from the parent OBO structure to a transition-state region where O_2 elimination can occur. Some B^+ is observed with approximately the same appearance energy as the main BO^+ channel. The competition between these channels makes analysis of the $BO^+ + O$ threshold somewhat ambiguous.

Given that thermochemistry appears to control the fragment branching, some energetic insight can be inferred directly from the branching patterns. In several cases we observe pairs of channels that differ only in which fragment carries the charge:

$$M^+ \rightarrow A^+ + B$$

$$\rightarrow A + B^+$$

As the fragments separate, we expect that the charge will largely end up on the fragment with the lower ionization energy (IE). If the IEs are similar, both pairs of channels will be observed, but if the difference is large, we expect significant signal only for the lower energy fragment pair. On the basis of this assumption, we can infer relationships between IEs for a number of B_nO_m species, and these are summarized in Table 4. In many cases these are not surprising and agree with literature thermochemistry. In others, the literature values are inconsistent with our results or no literature values are available.

One notable example is B_2O_3. Our fragmentation branching for $B_3O_4^+$ indicates that IE(B_2O_3) < IE(BO), whereas existing literature values[20] give an IE for B_2O_3 (13.56 eV) that is larger than that for BO (13.0 eV). Our G2 calculations, however, support this interpretation of our experimental results, and our hypothesis of thermodynamic control, i.e., the G2 IE for B_2O_3, 12.81 eV, is less than the G2 IE for BO, 13.01 eV.

Another example is B_2O_2. The fragmentation branching observed for $B_3O_3^+$ suggests that IE(B_2O_2) < IE(BO), whereas existing literature values[20] give an IE for B_2O_2 (13.58 eV) that is larger than that for BO (13.0 eV). Again the G2 calculations agree with the experimental prediction. The calculations predict the most stable $B_2O_2^+$ isomer ($BOBO^+$) is 11.82 eV higher in energy than the most stable form of B_2O_2 (OBBO), which is less than our calculated IE for BO, 13.01 eV. In all cases except for BO_2^+, the dominant product channel is the thermodynamically favored channel predicted by the G2 calculations.

Fragmentation Threshold Energies and Relation to Theory. The CID experiments show that BO_2^+ is the most stable and B_2O^+ the least stable cluster studied. The stability of the boron oxide clusters plotted as a function of the cluster size (Figure 2) exhibits an oscillating pattern typical for most size dependence cluster studies,[9,18] and the cluster stability clearly is strongly anticorrelated to the B:O ratio. As expected maximum stability is promoted by increasing the possibility for BO bonding.

Table 1 gives the best fit dissociation threshold extracted as discussed above, along with the associated value of the "*n*" parameter. Also given are the G2 dissociation energies. Note that the experimental uncertainties are abnormally large for these oxide cluster ions. This results from the fact that the fragmentation cross sections are unusually small (at maximum, only a few percent of the collision cross sections) and rise rather slowly from threshold. This suggests that collisional energy transfer is particularly inefficient for these clusters. The result is a larger-than-usual uncertainty in picking the best fit in the near-threshold energy range because the signal rises very slowly out of the noise. To give a clearer idea of which experimental dissociation threshold (E_0) values agree/disagree with the calculated dissociation energies, Figure 1 plots the best fits obtainable using the ab initio E_0 values.

For BO^+ there is an apparent discrepancy between the experimental and calculated E_0; however, as Figure 1 shows, the "best" and "theory" fits are similar. BO^+ has an anomalously small CID cross section, and the data are not good enough to justify concluding that the discrepancy is real. Similarly for B_2O^+, the 0.6 eV difference between the best fit E_0 and the ab initio value is within the combined uncertainties of the experiment and theory.

For BO_2^+ the best fit experimental E_0 (4.75 eV) is significantly lower than the calculated E_0 (5.60 eV), and in this case the difference is clearly outside the experimental uncertainty. There is a singlet excited state of BO_2^+ calculated to lie 0.6 eV (13.8 kcal/mol) above the triplet ground state, and if this could dissociate into ground-state products ($BO^+(^1\Sigma) + O(^3P)$), that would give a threshold close to the experimental value. Given that we use helium as our buffer gas, it would not be surprising if some singlet BO_2^+ survived in our ion beam. On the other hand, for light atoms and argon as the collision gas, it is far from obvious that the singlet−triplet dissociation can occur with measurable intensity.

Again for $B_2O_2^+$ there is nearly a 1 eV difference between the experimental best fit E_0 (3.15 eV) and the ab initio E_0 (4.10 eV). The experimental data is good enough that it is clear that the best "fit to theory" does not adequately reproduce the threshold behavior. As already noted, we considered the possibility that the ion beam might have significant contamination from a higher energy cyclic isomer, which would give a dissociation energy close to the experimental value. However, due to the small barrier for isomerization to the ground-state isomer, our calculations suggest it is unlikely the contribution from cyclic $B_2O_2^+$ could be greater than 10^{-4}—well below our sensitivity. A more likely candidate for these results is the next higher energy isomer, linear $OBBO^+$, which lies 1.88 eV above the ground-state isomer and 2.22 eV below the $B^+ + BO_2$ dissociation products. While 2.22 eV is below the measured threshold of 3.15 eV, the products likely cannot be reached without a substantial barrier. The measured threshold probably reflects either a barrier for isomerization to the low-energy $BOBO^+$ isomer or a transition state leading directly to $B^+ + BO_2$. A large (≥3.15 eV) barrier to isomerization is also the condition necessary for trapping of the high-energy isomer in our beam during the cooling process. The heat of formation of the $OBBO^+$ ion has actually been determined experimentally from the photoelectron spectrum of OBBO, the ground-state isomer of the neutral. The measured (adiabatic) IE of 13.58 eV[21] is in reasonable agreement with our calculated IE of 13.70 eV.

For $B_2O_3^+$, the experimental and ab initio E_0 values are in nearly perfect agreement. This is also a case where no low-lying isomers are expected to exist. $B_3O_3^+$ is another case where it is not possible to fit the experimental data with the E_0 value from the calculations. The experimental E_0 is over 1 eV lower than the calculation. As with all the oxides with B:O ratio equal to or greater than unity, several low-lying isomers are likely. The calculations find the $OBBOBO^+$ structure to be most stable, but $OBOBOB^+$ and a structure with a four-membered ring are both calculated to be within ~1 eV of the ground state. A small mixture of one or both could conceivably explain the lower experimental E_0. Our estimate of the possible contamination by the cyclic isomer for $B_3O_3^+$ is far below the level required to be experimentally observable. As discussed above, however, linear $OBOBOB^+$ isomer contamination is possible because this isomer lies only 0.58 eV above $OBBOBO^+$, and there likely is a large barrier separating the two linear isomers. The calculated 2.62 eV threshold for $OBOBOB^+$ dissociation is, however, still above the experimental threshold of 2.0 eV.

For $B_3O_4^+$ both intuition and the ab initio calculations suggest an $OBOBOBO^+$ lowest energy structure. However, as we found for both $B_2O_2^+$ and $B_3O_3^+$, there is also an isomer containing a four-membered BOBO ring lying about 1 eV higher in energy. For the $B_2O_2^+$ radical, the cyclic isomer is about 0.8 eV above the linear isomer, while for both $B_3O_3^+$ and $B_3O_4^+$ closed shell species, the cyclic isomer lies about 1.1 eV above the corresponding linear isomer. There is a substantial discrepancy between the experimental E_0 (4.25 eV) for $B_3O_4^+$ and that derived from the calculations (6.4 eV). Dissociation of the

TABLE 4: Comparisons of the Ionization Energies of Boron Oxide Cluster Ions

parent oxide cluster	IE relations inferred	literature IE relations[a]	G2 IE relations
B_2O^+	IE(BO) ≫ IE(B)	IE(BO) = 13.0eV IE(B) = 8.298eV consistent	IE(BO) = 13.01eV IE(B) = 8.20eV
$B_2O_2^+$	IE(BO_2) > IE(B)	IE(BO_2) = 13.5eV consistent	IE(BO_2) = 12.98eV
$B_2O_3^+$	IE(BO) ≈ IE(BO_2)	consistent	IE(BO) ≈ IE(BO_2)
$B_3O_3^+$	IE(B_2O_3) ≫ IE(B)	IE(B_2O_3) = 13.56eV consistent	IE(B_2O_3) = 12.82eV
	IE(BO) > IE(B_2O_2)	IE(B_2O_2) = 13.58eV inconsistent	IE(B_2O_2) = 11.82eV
$B_3O_4^+$	IE(BO) > IE(B_2O_3) IE(BO_2) > IE(B_2O_2)	inconsistent inconsistent	

[a] Lias, S. G.; Bartmess, J. E.; Liebman, J. F.; Holmes, J. L.; Levin, R. D.; Mallard, W. G. *J. Phys. Chem. Ref. Data* **1988,** *17*, Suppl.1.

cyclic isomer would occur, according to the calculations, at the somewhat lower threshold of 5.3 eV, still about 1 eV above experiment. At this point, the origin of the disagreement is not clear.

Implications for FBOH Thermochemistry. Another unresolved discrepancy is the heat of formation of FBOH. In our studies of boron oxide cluster ion reactions with HF, one of the major product channels observed was elimination of neutral or ionic FBOH:

$$B_nO_m^+ + HF \rightarrow B_{n-1}O_{m-1}^+ + FBOH$$

$$\rightarrow B_{n-1}O_{m-1} + FBOH^+$$

Production of neutral FBOH is inferred from the $B_{n-1}O_{m-1}^+$ product, for which FBOH is the lowest energy neutral partner. In reaction with $B_3O_4^+$, both these channels are observed with nearly equal intensities and with substantial cross sections at low collision energies, indicating that both are exothermic. The observation that the reaction producing $B_{n-1}O_{m-1}^+$ (+ FBOH) is exoergic allows us to put an upper limit on ΔH_f(FBOH). Taking our calculated G2 ΔH_f values for $B_3O_4^+$ (−46.4 kcal/mol) and $B_2O_3^+$ (98.6 kcal/mol), this requires that ΔH_f(FBOH) < −210 kcal/mol. This compares poorly with the ab initio ΔH_f(FBOH) = ∼ −113 kcal/mol calculated by Soto[5] and Page.[4] Our CID results find $B_3O_4^+$ to be ∼49 kcal/mol less stable than predicted by the G2 calculations. If we use this to estimate $\Delta H_f(B_3O_4^+)$ = ∼5 kcal/mol, this still requires that ΔH_f(FBOH) < ∼−160 kcal/mol. In either case, the discrepancy with the ab initio value is way outside the range of errors normally associated with those calculations.

The idea that FBOH is considerably more stable than what the ab initio calculations suggest is supported by the observation that the ($B_{n-1}O_{m-1}^+$ + FBOH) and ($B_{n-1}O_{m-1}$ + $FBOH^+$) product channels have nearly equal intensity for reaction of $B_3O_4^+$ with HF. This suggests that IE(FBOH) ≈ IE(B_2O_3) = 12.9 eV.[6] The difference between ab initio ΔH_f values for FBOH and for $FBOH^+$ (the latter being consistent with our results) gives IE(FBOH) = ∼7.5 eV. If this were correct, it seems unlikely that we would see significant signal for the $B_{n-1}O_{m-1}^+$ + FBOH channel because the charge should overwhelmingly migrate to FBOH as the products separate.

V. Conclusions

Our CID and ab initio results help clarify some of the confusion in the thermochemical literature for small boron oxide oligomers. The experimental results are largely consistent with the ab initio calculations presented here, though there are some unresolved issues. On the basis of the ab initio energies and frequencies, it appears unlikely that the cluster ion beam has significant contamination from high-energy cyclic isomers, but high-energy linear isomers may contribute to the experimental results in some cases. Significant (and related) discrepancies between theory and experiment exist for $B_3O_4^+$ and for FBOH.

Acknowledgment. This work was supported by the Office of Naval Research, Mechanics and Energy Conversion Division (Richard S. Miller), under grants N00014-95-10696 and N00014-96-10045.

References and Notes

(1) Linder, D.; Napora, R.; Page, M. Manuscript in preparation.
(2) Smolanoff, J.; Lapicki, A.; Kline, N.; Anderson, S. L. *J. Phys. Chem.* **1995,** *99*, 16276.
(3) Brown, R. C.; Kolb, C. E.; Rabitz, H.; Cho, S. Y.; Yetter, R. A.; Dryer, F. L. *Int. J. Chem. Kinet.* **1991,** *23*, 957.
(4) Yetter, R. A.; Rabitz, H.; Dryer, F. L.; Brown, R. C.; Kolb, C. E. *Combust. Flame* **1991,** *83*, 43.
(5) (a) Page, M. *J. Phys. Chem.* **1989,** *93*, 3639. (b) Page, M., private communication.
(6) Soto, M. *J. Phys. Chem.* **1995,** *99*, 6540.
(7) Duan, X.; Linder, D.; Page, M.; Soto, M., *J. Mol. Struct.* (*THEOCHEM*), in press.
(8) Hanley, L.; Ruatta, S. A.; Anderson, S. L. *J. Chem. Phys.* **1987,** *87*, 260.
(9) Hanley, L.; Whitten, J. L.; Anderson, S. L. *J. Phys. Chem.* **1988,** *92*, 5803.
(10) Alexander, A. J.; Hogg, A. M. *Int. J. Mass Spectrom. Ion Processes* **1986,** *69*, 297.
(11) Frisch, M. J.; Trucks, G. W.; Head-Gordon, M.; Gill, P. M. W.; Wong, M. W.; Foresman, J. B.; Johnson, B. G.; Schlegel, H. B.; Robb, M. A.; Replogel, E. S.; Gomperts, R.; Andres, J. L.; Raghavachari, K.; Binkley, J. S.; Gonzalez, C.; Martin, R. L.; Fox, D. J.; Defrees, D. J.; Baker, J.; Stewart, J. J. P.; Pople, J. A. *Gaussian 92, Revision A*; Gaussian, Inc.: Pittsburgh, PA, 1992.
(12) Chase, M. W.; Davies, C. A.; Dowey, J. R.; Frurip, D. J.; McDonald, R. A.; Szverud, A. N. JANAF Thermochemical Tables, 3rd ed., *J. Phys. Chem. Ref. Data* **1985**, *14*.
(13) Storms, A.; Mueller, E. B. *J. Phys. Chem.* **1977**, *81*, 318.
(14) Ruscic, B.; Mayhew, C. A.; Berkowitz, J. *J. Chem. Phys*. **1988**, *88*, 5580.
(15) Schlegel, H. B.; Harris, S. J. *J. Phys. Chem.* **1994**, *98*, 8, 11178.
(16) (a) Roos, B. O.; Taylor, P. R.; Siegbahn, P. E. M. *Chem. Phys*. **1980**, *48*, 152. (b) Roos, B. O. *Ab Initio Methods in Quantum Chemistry*; Lawley, K. P., Ed.; Wiley: Chichester, England, 1987; p 399.
(17) Saxe, P.; Lengsfield, B. H.; Martin, R.; Page, M. *MESA* (*Molecular Electronic Structure Applications*); University of California, 1990.
(18) Sowa-Resat, M. B.; Hintz, P. A.; Anderson, S. L. J. *Phys. Chem.* **1995,** *99*, 10736 and references therein.
(19) Zhu, L.; Hase, W. L. A general RRKM program, QCPE 644, Quantum Chemistry Program Exchange, Indiana University.
(20) Lias, S. G.; Bartmess, J. E.; Liebmann, J. F.; Holmes, J. L.; Levin, R. D.; *J. Phys. Chem. Ref. Data*. **1988,** *17*, Suppl. 1.
(21) Ruscic, B. M.; Curtiss, L. A.; Berkowitz, J. *J. Chem. Phys.* **1984**, *80*, 3962.